


The Transition (vs ΔpK_a) from Triple Ions to Free Cations in Poor Protic Ionic Liquids Made from Weak Acids

To cite this article: Smit S. Rana and Allan L. L. East 2022 *ECS Trans.* **109** 11

View the [article online](#) for updates and enhancements.

 The Electrochemical Society
Advancing solid state & electrochemical science & technology


242nd ECS Meeting



Oct 9 – 13, 2022 • Atlanta, GA, US

Presenting more than 2,400 technical abstracts in 50 symposia



ECS Plenary Lecture
featuring
M. Stanley Whittingham,
Binghamton University
Nobel Laureate –
2019 Nobel Prize in Chemistry





The Transition (vs ΔpK_a) from Triple Ions to Free Cations in Poor Protic Ionic Liquids Made from Weak Acids

Smit S. Rana and Allan L. L. East

Department of Chemistry and Biochemistry, University of Regina, Regina, SK S4S0A2,
Canada

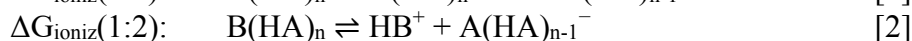
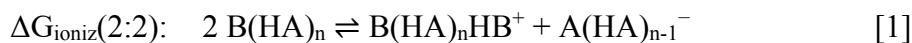
In mixtures of amines with carboxylic acids, the limited ionicity at 1:1 stoichiometric mixtures is due to insufficient ionization or ion pairing in low-dielectric environments. Higher conductivities have historically been seen at roughly 4:1 acid/base mixing ratios, where simulations have revealed large (and thus more stable) ions: homoassociated anions $(AH)(AH)(A^-)(HA)(HA)$ and cationic triple ions $(BH^+)(AH)(A^-)(HA)(HB^+)$. Recent work in understanding the Gibbs energies for degree-of-ionization equilibria hints that there may be an onset, for systems with an acid-base pK_a difference increasing towards 10, for the formation of free (unpaired) protonate-amine cations BH^+ . The transition with increasing ΔpK_a is explored in this work, to aid in the prediction of ionicity and conductivity of protic ionic liquids.

Introduction

Use of a Walden plot (log of molar conductivity versus log of reciprocal viscosity) to recognize cases of limited ionicity in ionic liquids was pioneered by Angell and co-workers, with two papers in chemistry journals in 2003 on aprotic (1) and protic (2) ionic liquids. [Here, a protic ionic liquid or PIL refers to an IL made by proton transfer from acid to base (3), not ILs with “active” protons.] Limited ionicity in the aprotic cases might be described by an activity coefficient or by an ion-pairing equilibrium. In the protic cases, an additional possibility for limited ionicity could be incomplete protonation of the base by the acid, described by a proton-transfer equilibrium. Whatever the reason, Angell and co-workers observed that limited ionicity in PILs seemed to occur in systems of low proton transfer strength, i.e. those with $\Delta pK_a < 10$, where ΔpK_a is the difference in logarithms (pK_a) of the aqueous acidity constants (K_a) of the acid HA and the protonated base HB^+ (2).

East, Johnson, and co-workers (4-6) have been studying the limited ionicity of classic systems of amines with carboxylic acids (7-16), with $\Delta pK_a = 0-6$. Such systems have a wealth of published data, including density and viscosity data for both stoichiometric and non-stoichiometric mixing mole ratios $n = x_A/x_B$. This data has been extremely helpful for the development of what they called kite theory (4) to describe PIL liquid structure, limited ionicity, and conductivity. “Kite” refers to the ion-pair structures and a fully ion-paired reference state in the theory.

One interesting aspect in the kite theory to date is the assumption that the cation contributing to conductivity is not BH^+ but “two-headed kites,” i.e. translating *triple-ion* complexes $(BH^+)(AH)_x(A^-)(HA)_y(HB^+)$. This assumption was based on *ab initio* molecular dynamics simulations of poor PILs at mixing ratios from 1 to 5 (4,5). Recent work (6) on improving the prediction of association Gibbs energies, including ion-pair association, have revealed that this assumption may lead to underprediction of ion concentration for systems with ΔpK_a near or above 6, and that free BH^+ becomes relevant at some ΔpK_a threshold. Hence, we report here on our recent use of these new functions for association Gibbs energies to search for ΔpK_a thresholds for the relevance of Eq. [2] as an additional contributor, beyond Eq. [1], for autoionization of the ion pairs (“kites”) in PILs:



This report principally presents plots of predicted ion concentrations versus acid/base mixing ratio n and acid/base proton-transfer strength ΔpK_a . Initially we present results from each of the above autoionization models individually. We finish by presenting results from a full coupling of both possibilities, allowing for the possible presence of both monomer and triple-ion cations. Of particular interest will be learning the ΔpK_a ranges for which either, or both, of Eqs. [1] and [2] would be appropriate for describing the autoionization.

Theory

Ion concentration predictions are computed from equations below. We assume standard temperature and pressure (298.15 K, 1 atm) throughout.

Primary variables are the mixing ratio n and the acid/base proton transfer strength ΔpK_a . Secondary variables, which depend on n and the identities of the acid and base, are the dielectric constant ϵ and mass density ρ . For ϵ , known to depend heavily on mixing ratio n but more mildly on acid/base identity, we tested the artificial fixed-dielectric choice of $\epsilon = 28$ and the more realistic and typical $\epsilon(n)$ choice of

$$\epsilon = 3 + 17ne^{-0.08n^2} \quad [3]$$

which fits reasonably well the data of Orzechoski et al. for mixtures of trimethylamine and propionic acid (13). This varying dielectric constant is highest for n between 2 and 3, due to large dipoles of the ion-pair “kites,” $B(HA)_n$. At $n > 3$, although these individual dipoles should get even larger, the dipole density (concentration) decreases and becomes a limiting factor for ϵ . For ρ , we employed two specific functions which fit known data (9,10), as well as an averaged “typical” density when making property plots versus arbitrary ΔpK_a :

$$\rho_{\text{PYR/HAc}} (\text{g mL}^{-1}) = 1.08 - \frac{0.06}{n} \quad [4a]$$

$$\rho_{\text{TEA/HAc}} (\text{g mL}^{-1}) = 1.06 - \frac{0.16}{n} \quad [4b]$$

$$\rho_{\text{typical}} (\text{g mL}^{-1}) = 1.07 - \frac{0.11}{n} \quad [4c]$$

Intermediate quantities in the prediction of ion concentration are the initial kite (ion-pair) molar masses M and concentration c , association radii r , induced dipole moments μ , association Gibbs energies ΔG_A , ionization Gibbs energies ΔG_{ioniz} of eqs. 1 and 2, and equilibrium constants K_A and K_{ioniz} . The additional equations for these were

$$M_{\text{PYR/HAc}} (\text{g mol}^{-1}) = 79 + 60 n \quad [5a]$$

$$M_{\text{TEA/HAc}} (\text{g mol}^{-1}) = 101 + 60 n \quad [5b]$$

$$M_{\text{typical}} (\text{g mol}^{-1}) = 90 + 60 n \quad [5c]$$

$$c = \frac{\rho}{M} \quad [6]$$

$$r_{n+} = r_0 + r_1 n \quad [7]$$

$$r_0 (\text{\AA}) = (4.08 - 0.33 \ln \varepsilon - 2.29 e^{-0.02 \Delta pKa}) \quad [8]$$

$$r_1 (\text{\AA}) = (4.21 - 0.14 \ln \varepsilon - 2.88 e^{-0.02 \Delta pKa}) \quad [9]$$

$$\mu_{n,+} = \mu_1 n + \mu_2 n^2 \quad [10]$$

$$\mu_1 (\text{\AA} e_0) = (2.90 + 0.13 \ln \varepsilon - 2.49 e^{-0.02 \Delta pKa}) \quad [11]$$

$$\mu_2 (\text{\AA} e_0) = (0.27 - 0.00 \ln \varepsilon - 0.00 e^{-0.02 \Delta pKa}) \quad [12]$$

$$\Delta G_{A,+} (\text{kcal mol}^{-1}) = \frac{-N_{AVO}}{4\pi\varepsilon_0\varepsilon} \left(\frac{q_+\mu_{n,+}}{r_{n+}^2} + \frac{q_+q_-}{r_{n+}} \right) - T\Delta S = \frac{-332}{\varepsilon} \left(\frac{\mu_{n,+}}{r_{n+}^2} + \frac{1}{r_{n+}} \right) + 5 \quad [13]$$

$$\Delta G_{A,+0} (\text{kcal mol}^{-1}) = \frac{-N_{AVO}}{4\pi\varepsilon_0\varepsilon} \left(\frac{q_+\mu_{n,+}}{r_{n+}^2} \right) - T\Delta S = \frac{-332}{\varepsilon} \left(\frac{\mu_{n,+}}{r_{n+}^2} \right) + 5 \quad [14]$$

$$q_+ = q_- = e_0 = 1.602 \times 10^{-19} \text{ Coulomb} \quad [15]$$

$$N_{AVO} e_0^2 / (4\pi\varepsilon_0) = 332 \text{ \AA kcal mol}^{-1} \quad [16]$$

$$\Delta G_{\text{ioniz}}(2:2) = \Delta G_{A,+0} - \Delta G_{A,+} \quad [17]$$

$$\Delta G_{\text{ioniz}}(1:2) = -\Delta G_{A,+} \quad [18]$$

$$K = e^{-\Delta G/RT} \quad [19]$$

Eqs. [7-14] were recently derived (6) from fitting to *ab initio* data that happened to reproduce experimentally derived $\Delta G_{\text{ioniz}}(2:2)$ for the pyridine/acetic acid system ($\Delta pK_a = 0.5$) under the assumption that $[\text{BH}^+] = 0$.

Finally, ion concentrations were determined from starting ion-pair concentration c (Eqs. [4-6]) and equilibrium constants (Eqs. [7-19]), using the following mass-balance equations. Let x = anion concentration and $i = 2x$ be total ion concentration. Assuming only 2:2 autoionization (Eqs. [1, 13, 19]), $K = (x)^2/(c-2x)^2$, leading to

$$i_{2:2} = c\sqrt{K_{2:2}}/(1 + 2\sqrt{K_{2:2}}) \quad [20]$$

Assuming only 1:2 autoionization (Eqs. [2, 14, 19]), $K = (x)^2/(c-x)$, leading to

$$i_{1:2} = -K_{1:2} + \sqrt{K_{1:2}^2 + 4cK_{1:2}} \quad [21]$$

Results and Discussion

Single Equilibrium Results, versus Acid/Base Mixing Ratio n

Figure 1 shows results for total ion concentration predictions from each of the ionization models individually (2:2 vs 1:2, generating triple-ion cations vs free BH^+ cations, respectively), plotted versus acid/base mixing ratio n . The ΔpK_a values used are 0.5 for pyridine/acetic acid and 6.0 for triethylamine/acetic acid. Results from both dielectric constant choices discussed in the Methods section are shown: constant $\epsilon = 28$ results in dashed lines, and the more realistic $\epsilon(n)$ of Eq. [3] in solid lines. For B = pyridine ($\Delta\text{pK}_a = 0.5$, left-hand plot), more ions are predicted from the 2:2 model (black) than the 1:2 model (grey), but for B = trimethylamine ($\Delta\text{pK}_a = 6.0$, right-hand plot), the opposite is true for acid/base mixing ratios $n = 2-4$. Thus, the ΔpK_a onsets, or crossover points, at which the 1:2 ion generation becomes dominant, appear to be below 6 for $n = 2-4$, but above 6 for the commonest case of $n = 1$, as well as $n > 4$.

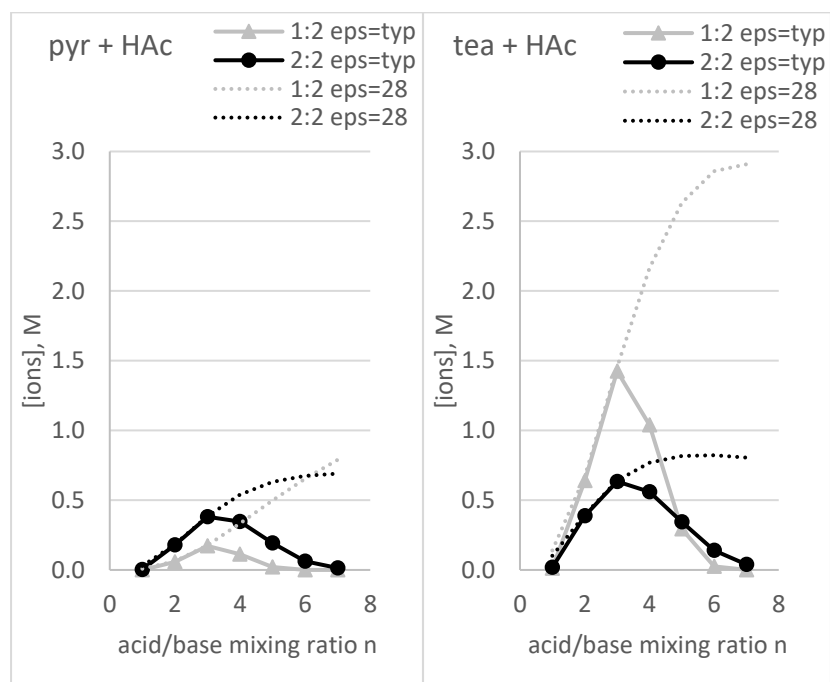


Figure 1. Total ion concentration vs n , comparing ionization models.

Figure 2 plots the Gibbs energy difference $\Delta G_{\text{diff}} = 2 \Delta G_{\text{ioniz}}(1:2) - \Delta G_{\text{ioniz}}(2:2)$. This is the Gibbs energy for the triple-ion fragmentation reaction $\text{B}(\text{HA})_n\text{HB}^+ \rightarrow 2 \text{HB}^+ + \text{A}(\text{HA})_{n-1}^-$. Comparing the dashed curves to the solid ones, one can see that the strongly parabolic dependence of ΔG_{diff} upon mixing ratio n in the more realistic solid curve is due to the strong variation of ϵ upon n . There is also dependence on the ΔpK_a (the left vs right plots), and in the right-hand plot we see negative values predicted for $n = 3$ and $n = 4$: not just a contribution but a *preference* for triple-ion fragmentation is predicted in these conditions ($\Delta\text{pK}_a = 6$).

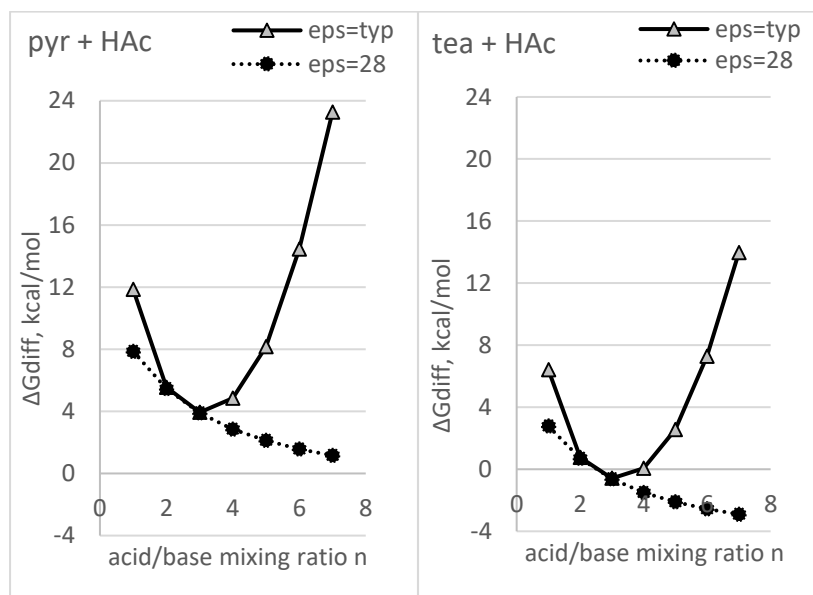


Figure 2. Triple-ion fragmentation Gibbs energy (ΔG_{diff}) vs n .

Single-Equilibrium Results, versus ΔpK_a

Figure 3 plots the total ion concentration predictions versus ΔpK_a , assuming $c = c_{\text{typ}} = \rho_{\text{typ}}/M_{\text{typ}}$ in Eq. 6. Only data using “realistic ϵ ” is shown (using Eq. [3]). These plots reveal the ΔpK_a crossover points beyond which the 1:2 ionization hypothesis generates more ions than the 2:2 ionization. These crossover points are listed in Table I. We first note that they all lie below $\Delta pK_a = 10$. Secondly we note that pairing acetic acid with *aromatic* amines, generally giving $\Delta pK_a < 3$, are thus generally predicted to ionize via the 2:2 model (triple-ion cations) at all n as we had assumed (4,5), but pairing acetic acid with *aliphatic trialkylamines*, generally giving $\Delta pK_a > 3$, are now predicted to have a mixture of cations (BH^+ and triple ions) at $n > 1$ ratios.

TABLE I. ΔpK_a Crossover Points, Past Which Eq. [1] Generates More Ions Than Eq. [2].

Mixing Ratio n	ΔpK_a
1	8.8
2	3.8
3	2.6
4	3.5
5	6.8

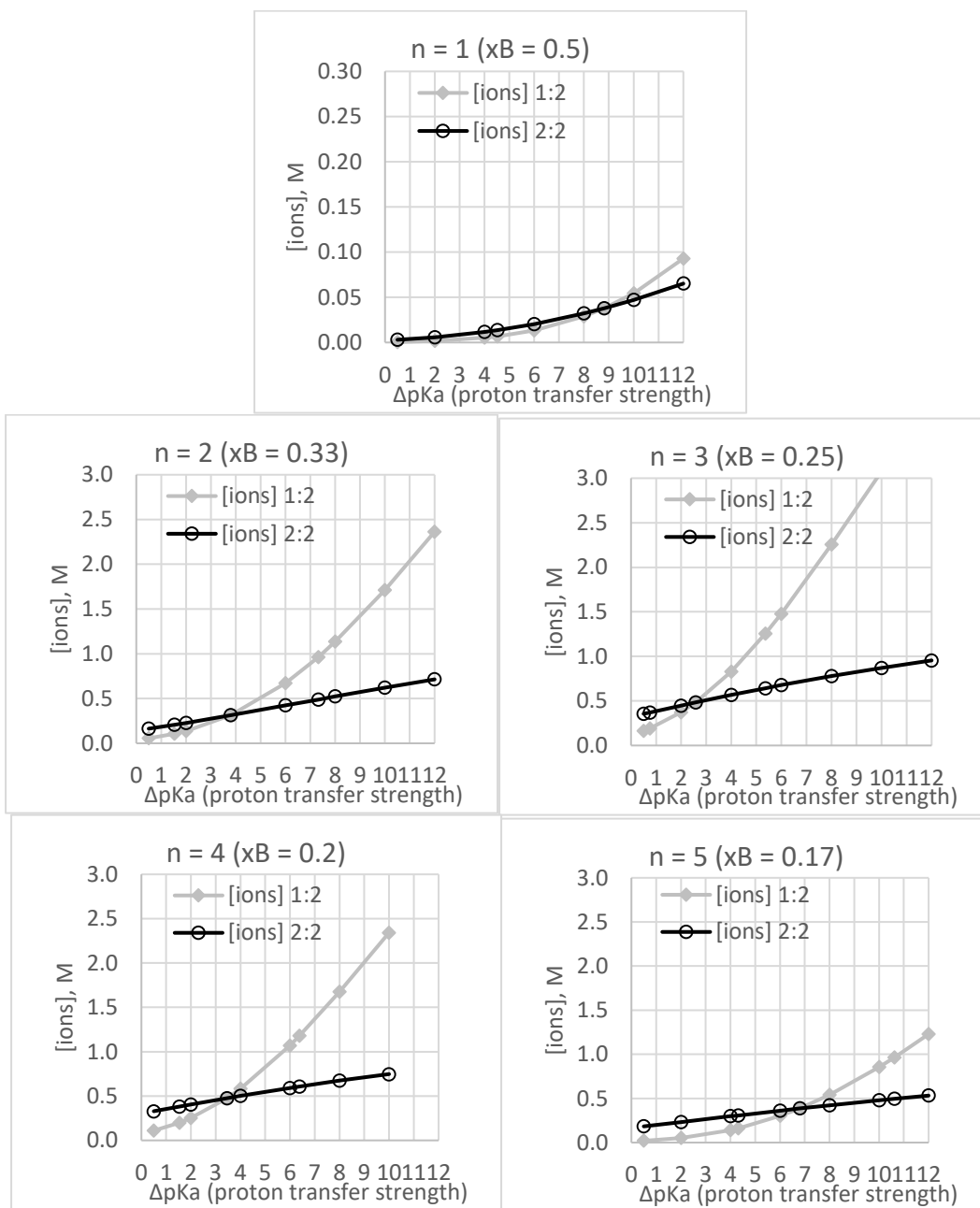


Figure 3. Total ion concentration vs ΔpK_a , comparing ionization models.

Figure 4 plots the triple-ion fragmentation ΔG_{diff} versus ΔpK_a , using “realistic ε ” data only. The crossover points in Table 1 occur when ΔG_{diff} has become “sufficiently small,” but this varies: roughly $+5 \text{ kcal mol}^{-1}$ for $n=1$ but closer to $+2 \text{ kcal mol}^{-1}$ for $n = 2-5$. Hence, the fragmentation ΔG_{diff} value does not have to drop to zero for the 1:2 model to generate more ions than the 2:2 model.

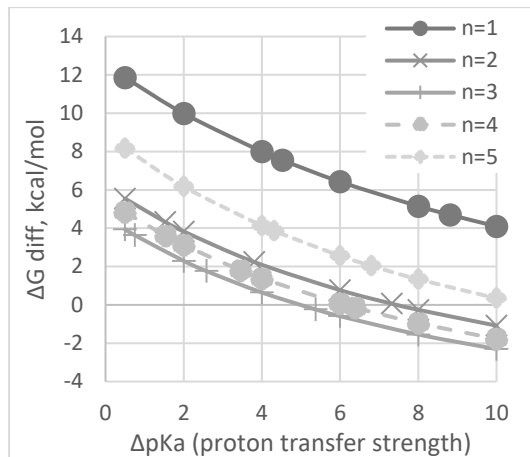


Figure 4. Triple-ion fragmentation Gibbs energy vs ΔpK_a for different values of n .

Coupled-Equilibrium Results

An exact solution for the ion concentrations arising from properly coupling Eqs.[1] and [2] is achievable from values of two equilibrium constants P and Q and the initial kite concentration c , by solving the following cubic equation for B :

$$B^3 + (Q + c)B^2 + PQB - PQc = 0 \quad [22]$$

$$P = 1/K_{A,+} = e^{+\Delta G_{A,+}/RT} \quad [23a]$$

$$Q = 1/K_{A,+0} = e^{+\Delta G_{A,+0}/RT} \quad [23b]$$

The physically relevant solution of the cubic equation for B , from one of the three general cubic-equation solutions as given by Wolfram MathWorld (17), is

$$B = 2(\sqrt{-Q})\cos(\theta/3) - (a_2/3) \quad [24]$$

$$\theta = \arccos(\mathbb{R}(-Q)^{-3/2}) \quad [25a]$$

$$Q = (3a_1 - a_2^2)/9 \quad [25b]$$

$$\mathbb{R} = (9a_1a_2 - 27a_0 - 2a_2^3)/54 \quad [25c]$$

$$a_0 = -PQc \quad [25d]$$

$$a_1 = PQ \quad [25e]$$

$$a_2 = Q + c \quad [25f]$$

The resulting ion concentrations are

$$[\text{BH}^+] = B \quad [26]$$

$$[\text{A}(\text{HA})_{n-1}^-] = x = \frac{BPQ}{PQ - B^2} \quad [27]$$

$$[\text{B}(\text{HA})_n\text{HB}^+] = y = \frac{BPQ}{PQ - B^2} - B \quad [28]$$

$$i = 2x = 2\left(\frac{BPQ}{PQ - B^2}\right) \quad [29]$$

and are plotted in Figure 5 as function of ΔpK_a , for several values of n . (The ΔpK_a and n affect the values of c and the ΔG_A in Eqs. [22,23].)

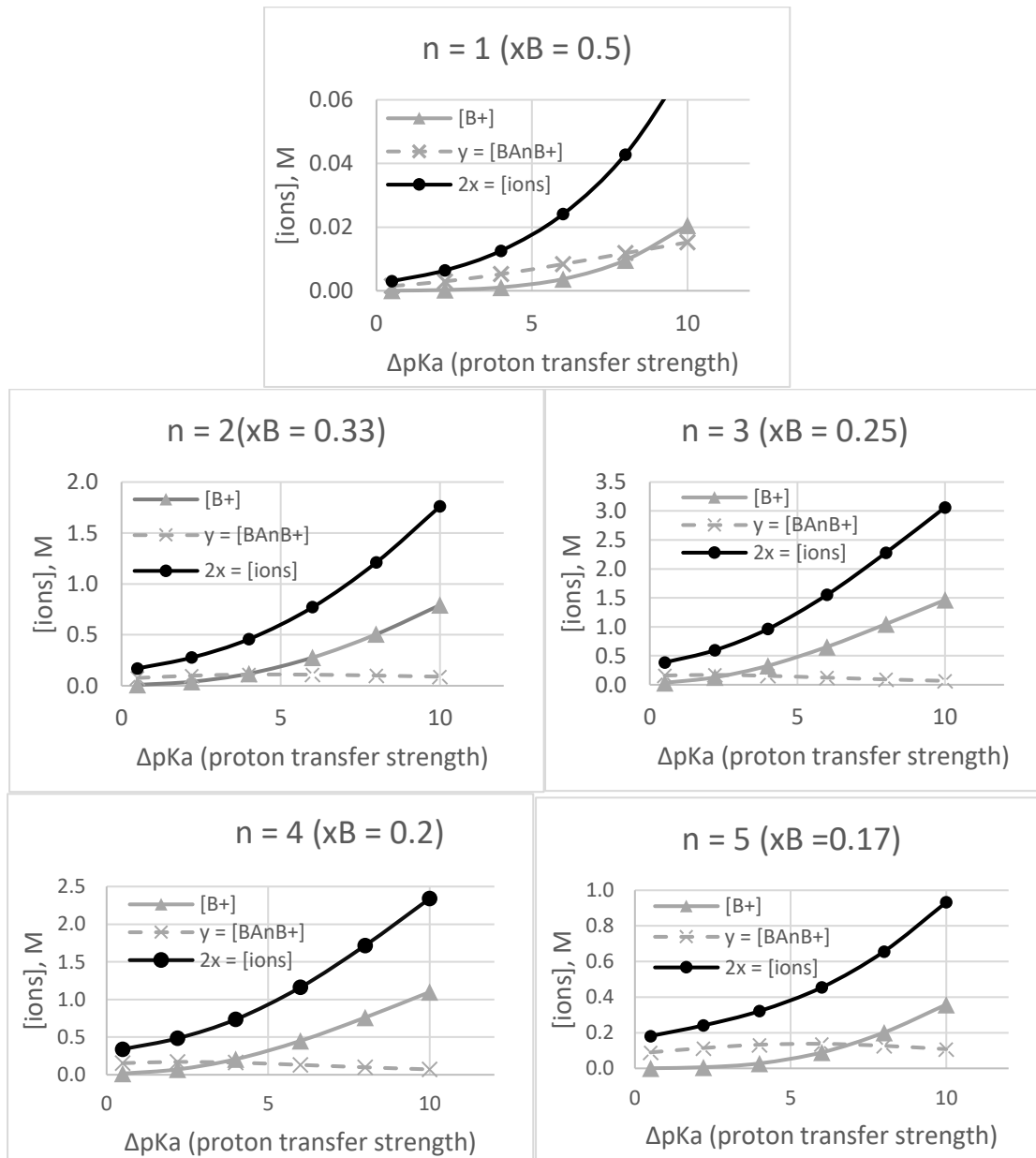


Figure 5. Predicted ion concentrations vs ΔpK_a from coupled equilibria, using “typical” $\epsilon(n)$ and $c(n)$ (Eqs. [3,4c,5c]); each plot covers a particular acid/base mixing ratio n .

The ΔpK_a crossover locations, at which $[BH^+] = [B(HA)_nHB^+]$, are similar to what were found from single-equilibrium calculation (Table I). The transition region, the *range* of ΔpK_a values for which both cation types are significantly contributing to total ion concentration i (i.e. the range where solving coupled equilibria would be worth the effort), is not small; said another way, the transition from triple ions to single ions with rising ΔpK_a is not sudden. These ranges, which depend on n , are quantified in Table II as the ranges where both cation types contribute $> 20\%$ to total cation concentration ($> 10\%$ to total ion concentration).

TABLE II. Predicted ΔpK_a Ranges Where Each Cation Type Contributes $> 10\%$ of Total Ions.

Mixing Ratio n	ΔpK_a Range
1	4.5 - 16.1
2	1.5 - 7.3
3	0.7 - 5.4
4	1.5 - 6.4
5	4.3 - 10.6

These predictions depend not only on the accuracy of the predicted ΔG_A from Eqs. [7-14] from ref. (6), but also in the $\varepsilon(n)$ approximation in Eq. (3). One indication of questionable accuracy in the above coupled-equilibria predictions is in the very low ion concentrations predicted for $n = 1$ (the common 1:1 mixing ratio), even at $\Delta pK_a = 10$ where Angell's Walden plots show rather good ionicity (2). Figure 6 extends the predictions above to very large ΔpK_a values, to see where i starts to approach Eq. [2] full-ionicity values of $2c = \{12.8, 9.7, 7.7, 6.3, 5.4\}$ mol L⁻¹ for $n = \{1, 2, 3, 4, 5\}$, respectively. Degree of ionization measured according to Eq. [2] would be $i/2c$. The “ ΔW ” data assembled by Angell and co-workers in Figure 10 of Ref. (2) indicate that, if the limited ionicity (ΔW) were due only to degree of ionization, $i/2c$ should have been $\{0.001, 0.01, 0.1\}$ at $\Delta pK_a = \{1, 2, 4\}$. Since $2c$ is roughly 14 mol L⁻¹, this means i should have been $\{0.014, 0.14, 1.4\}$ mol L⁻¹ at $\Delta pK_a = \{1, 2, 4\}$. Our predictions for i in Fig. 5 and 6 are thus seen to be good for $\Delta pK_a = 0-1$ (i.e. pyridine + acetic acid, where the 2:2 ionization assumption is fine), but not rising quickly enough at $\Delta pK_a > 2$. More data (re-derived experimental ΔG_{ioniz} for the $\Delta pK_a = 6$ TEA + acetic acid mixtures, and B3LYP ΔG_{ioniz} data for $\Delta pK_a > 6$) would be beneficial to see if the thermodynamic functions (Eqs. [7-14]) require improvement for $\Delta pK_a \sim 6$ and above.

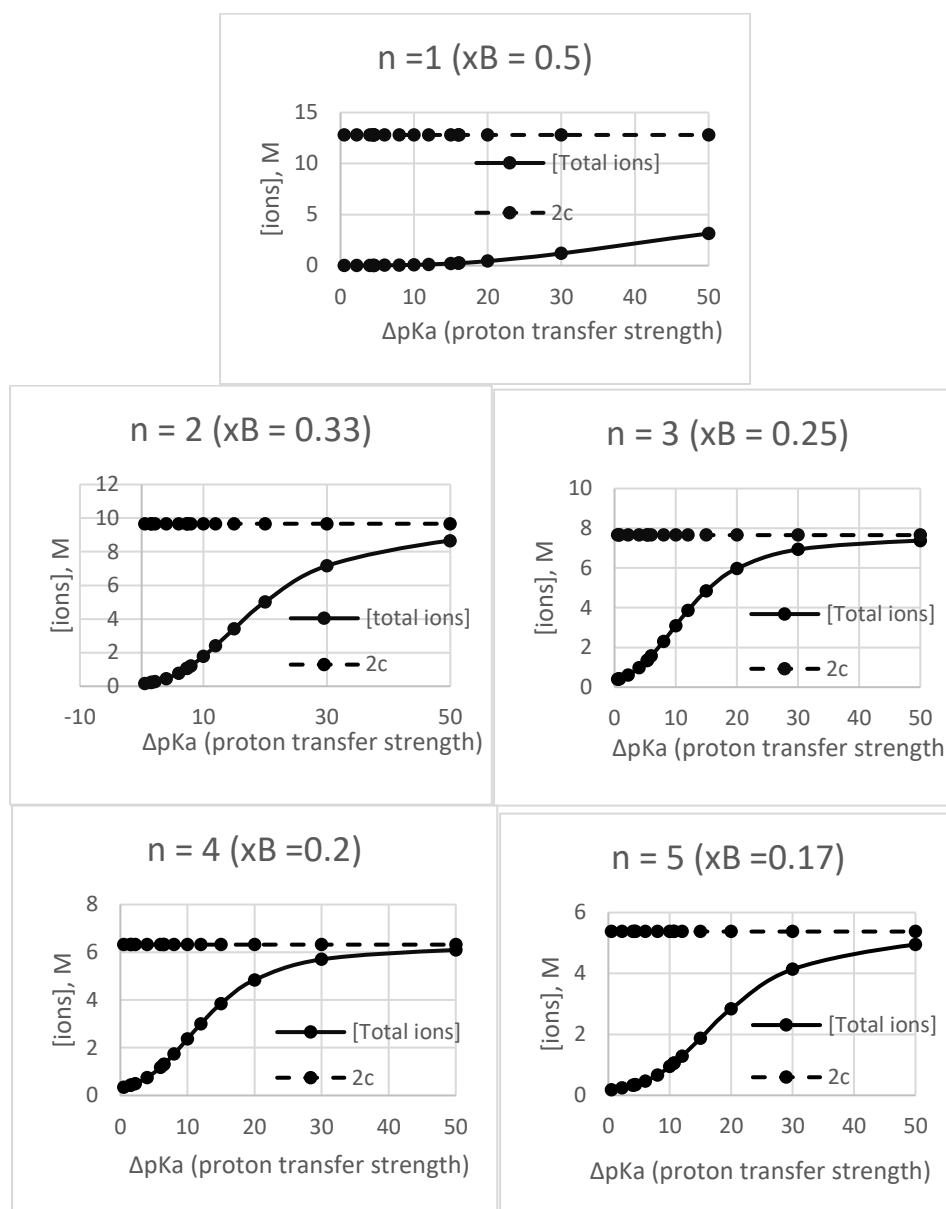


Figure 6. Predicted ion concentrations as in Fig. 5 but for larger ΔpK_a values.

Conclusions

Using the new association Gibbs energies of ref. 6 (Eqs. [7-14] here), we have explored the conditions where the dominant PIL autoionization (ion-depairing) equilibrium changes from Eq. [1] (generating triple-ion cations) to Eq. [2] (generating free monomer cations). For stoichiometric ($n = 1$, i.e. 1:1 acid + base) protic ionic liquids (PILs), the previously assumed Eq. [1] should be *coupled* with Eq. [2] when $4.5 < \Delta pK_a < 16$, and *replaced* by Eq. [2] when $\Delta pK_a > 16$. For acid-rich mixtures ($n > 1$), Table II has the appropriate ranges. Comparison with the “ ΔW ” limited-ionicity data assembled by Angell and co-workers (2) indicates that the predicted total ion concentrations here are likely too low for $\Delta pK_a > 2$, even from coupled-equilibria predictions, making these ΔpK_a ranges for the use of coupled

equilibria rather tentative. Future work is planned to (i) improve the association Gibbs energies (ΔG_A) for $\Delta pK_a > 2$, by generating more ΔG_A data and refitting, and (ii) using the improved ΔG_A to replace the Fuoss-equation ion concentration formulae in kite theory (4) for better prediction of limited ionicity and conductivity in protic ionic liquids.

Acknowledgements

The work was supported by NSERC Canada (RGPIN-2017-06247).

References

1. W. Xu, W., E. I. Cooper, and C. A. Angell, *J. Phys. Chem. B.* **107**, 6170 (2003).
2. M. Yoshizawa, W. Xu, and C. A. Angell, *J. Am. Chem. Soc.* **125**, 15411 (2003).
3. T. L. Greaves and C. J. Drummond, *Chem. Rev.* **115**, 11379 (2015).
4. N. P. Aravindakshan, K. E. Gemmell, K. E. Johnson, and A. L. L. East, *J. Chem. Phys.* **149**, 094505 (2018).
5. D. O. Klapatiuk, K. E. Johnson, and A. L. L. East, *ECS Trans.* **98**(10), 149 (2020).
6. D. O. Klapatiuk, S. L. Waugh, and A. L. L. East, manuscript submitted for publication.
7. H. E. Patten, *J. Phys. Chem.* **6**, 554 (1902).
8. L. E. Swearingen and R. F. Ross, *J. Phys. Chem.* **38**, 1141 (1934).
9. V. K. Venkatesan and C. V. Suryanarayana, *J. Phys. Chem.* **60**, 777 (1956).
10. P. Huyskens, N. Felix, A. Janssens, F. Van den Broeck, and F. Kapuku, *J. Phys. Chem.* **84**, 1387 (1980).
11. F. Kohler, R. Gopal, G. Goetze, H. Atrops, M. A. Demiriz, E. Liebermann, E. Wilhelm, F. Ratkovics, and B. Palagyi, *J. Phys. Chem.* **85**, 2524 (1981).
12. K. Orzechowski, M. Pajdowska, J. Przybylski, J. Gliński, and H.A. Kolodziej, *Phys. Chem. Chem. Phys.* **2**, 4676 (2000).
13. K. Orzechowski, M. Pajdowska, K. Fuchs, U. Kaatze, *J. Chem. Phys.* **119**, 8558 (2003).
14. R. G. Treble, K. E. Johnson, and E. Tosh, *Can. J. Chem.* **84**, 915 (2006).
15. T. L. Greaves, A. Weerawardena, I. Krodkiewska, and C. J. Drummond, *J. Phys. Chem. B* **112**, 896 (2008).
16. K. M. Johansson, E. I. Izgorodina, M. Forsyth, D. R. MacFarlane, and K. R. Seddon, *Phys. Chem. Chem. Phys.* **10**, 2972 (2008).
17. Wolfram MathWorld website, <https://mathworld.wolfram.com/CubicFormula.html>